Organic & Biomolecular Chemistry

RSC Publishing

PAPER

View Article Online
View Journal | View Issue

Cite this: *Org. Biomol. Chem.*, 2013, **11**, 344

pH-tuned metal coordination and peroxidase activity of a peptide dendrimer enzyme model with a Fe(II)bipyridine at its core†

Piero Geotti-Bianchini, Tamis Darbre* and Jean-Louis Reymond*

Received 6th August 2012,
Accepted 7th November 2012

DOI: 10.1039/c2ob26551f

www.rsc.org/obc

Peptide dendrimer **BP1** was obtained by double thioether bond formation between 5,5′-bis(bromomethyl)-2,2′-bipyridine and two equivalents of peptide dendrimer **N1** (Ac-Glu-Ser)$_8$(*Dap*-Glu-Ala)$_4$(*Dap*-Amb-Tyr)$_2$*Dap*-Cys-Asp-NH$_2$ (*Dap* = branching 2,3-diaminopropanoic acid, Amb = 4-aminomethyl-benzoic acid). At pH 4.0 **BP1** bound Fe(II) to form the expected tris-coordinated complex [Fe^{II}(**BP1**)$_3$] (K_f = 2.1 × 10^{15} M^{-3}). At pH 6.5 a monocoordinated complex [Fe^{II}(**BP1**)] was formed instead (K_f = 2.1 × 10^5 M^{-1}) due to electrostatic repulsion between the polyanionic dendrimer branches, as confirmed by the behavior of three analogues where glutamates were partially or completely replaced by neutral glutamines or positive lysines. [Fe^{II}(**BP1**)] catalyzed the oxidation of *o*-phenylenediamine with H_2O_2 with enzyme-like kinetics (k_{cat} = 1.0 min^{-1}, K_M = 1.5 mM, k_{cat}/k_{uncat} = 90 000) and multiple turnover, while Fe^{2+} or [Fe(bipy)$_3$]$^{2+}$ were inactive. The labile coordination positions allowing coordination to H_2O_2 and to the substrate are likely responsible for the enhanced peroxidase activity of the metallopeptide dendrimer.

Introduction

Dendrimers are regularly branched, tree-like macromolecules that can be assembled from a variety of dendron building blocks. While dendrimers are conformationally flexible, their branched topology enforces a roughly globular shape leading to microenvironments near the dendrimer core and multivalency at the dendrimer periphery, which can be exploited to design functional systems in biology and in catalysis.[1] In the case of catalysis, microenvironment effects may enhance or modify the reactivity of key catalytic groups at the dendrimer core and enable substrate concentration or binding.[2] On the other hand, the multivalent display of functional groups at the dendrimer periphery may lead to enhanced catalytic potency and/or selectivity by cooperativity, *e.g.* enhanced enantioselectivity of tetravalent dendritic (Co)Salen complexes for epoxidation,[3] or increased activity for phosphate hydrolysis by multivalent dendritic zinc containing dendrimers.[4] Dendritic multivalent display also increases the molecular weight of small molecule catalysts and has been used to facilitate catalyst recycling.[5]

Peptide dendrimers developed in our group display functional amino acid side chains at their core, within the branches and at the dendrimer periphery in an "apple-tree" configuration favorable to design dendritic models for enzymes, glycoproteins, drug delivery and antimicrobial agents.[6] In particular, enzyme models for esterases displaying cooperativity between protonated and deprotonated histidine residues[7] and a model with a single catalytic site[8] showed a high rate enhancement for ester hydrolysis. Aldolase mimics with multiple proline residues were also developed.[9]

Here we report the synthesis of a peptide dendrimer with a 2,2′-bipyridine group in the core able to form a 1 : 1 complex with Fe(II), [Fe^{II}(**BP1**)], at pH 6.5 and a 3 : 1 complex, [Fe^{II}(**BP1**)$_3$], at pH 4. The iron coordination is most likely tuned by the accumulation of negative charges in the dendrimer periphery due to deprotonation of side-chain carboxylic functions.

Dendrimer [Fe^{II}(**BP1**)] catalyzes the oxidation of chromogenic *o*-phenylenediamine with hydrogen peroxide (Fig. 1).

In our first attempt to develop peptide dendrimers as ligands for metals, combinatorial libraries were screened with aquocobalamin.[10] This approach led us to characterize peptide dendrimer **N1** (Scheme 1) as a ligand to vitamin B_{12}. Cobalt coordination by the cysteine residue at the dendrimer **N1** core was accelerated by the presence of the multiple anionic glutamate residues in the outer dendrimer branches. Analogs of

Department of Chemistry and Biochemistry, University of Berne, Freiestrasse 3, CH-3012 Berne, Switzerland. E-mail: tamis.darbre@ioc.unibe.ch, jean-louis.reymond@ioc.unibe.ch

†Electronic supplementary information (ESI) available: SPPS and purification of peptide dendrimers, HPLC analyses and MS spectra of all ligands; full experimental details for titrations, NMR diffusion measurements and catalytic experiments; ^{1}H NMR of bipyridine dendrimer ligands and Fe(II)-complexes. See DOI: 10.1039/c2ob26551f

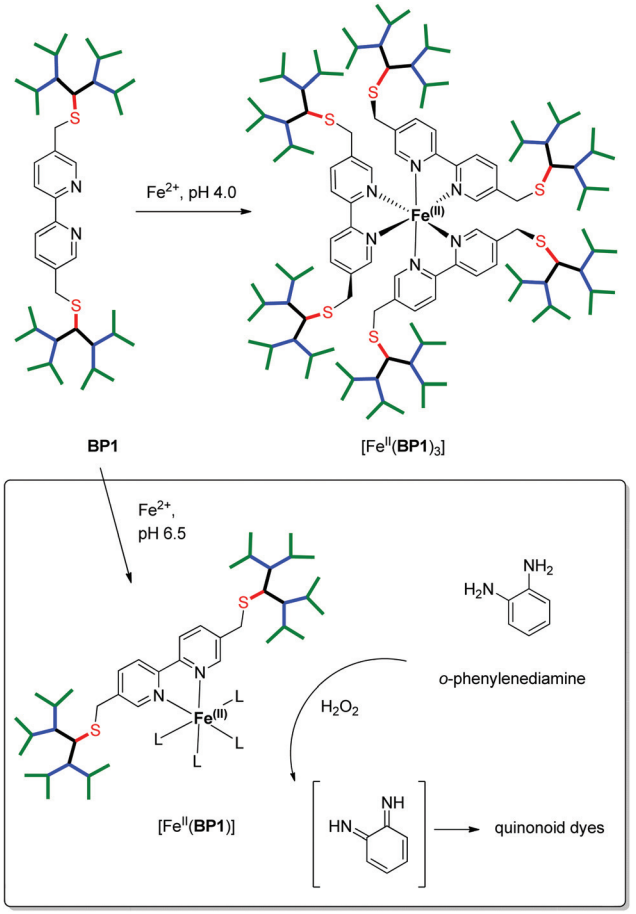

Fig. 1 A metallopeptide dendrimer peroxidase enzyme model (see also Scheme 1 for complete structural formula of peptide dendrimer **BP1**). Monodentate ligand L = H_2O or amino acid side chains such as carboxylate from glutamate.

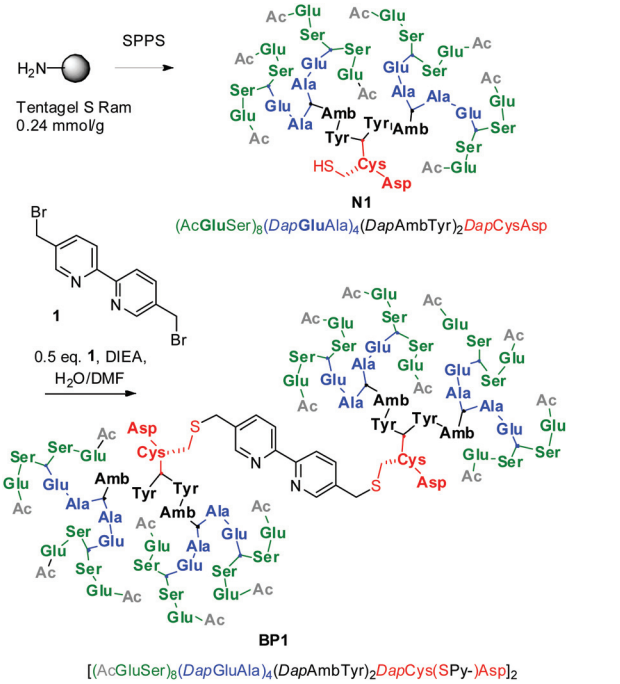

Scheme 1 Synthesis of bipyridine peptide dendrimer **BP1**. The branching diamino acid (●) is (*S*)-2,3-diaminopropanoic acid (Dap). Amb = 4-aminomethylbenzoic acid. Py = 5-methyl-2-pyridyl. The C-terminus at Asp is $CONH_2$.

dendrimer **N1** with cationic residues in the outer dendrimer branches did not bind to vitamin B_{12}.[11] A similar charge effect was observed for Fe(II) binding to second generation peptide dendrimers carrying a bipyridine ligand at the dendrimer focal point (bipy-dendrimers).[12] Thus, bipy-dendrimers with multiple glutamates in their periphery showed strong binding to Fe(II) and formed tricoordinated complexes, while bipy-dendrimers with arginine residues in their branches did not bind at all. Such control of metal coordination to bipyridine by remote charges had not been reported before despite the extensive metal coordination chemistry of bipyridines with various metal ions to form supramolecular assemblies,[13] bipyridine containing dendrimers[14] and peptide-appended bipyridine complexes.[15]

In the previous examples, Fe(II) coordination was determined by the nature of the amino acids in the peptide dendrimers, which determined the charge density. We hypothesized that the coordination control could also be possible with the same peptide dendrimer by modulating the pH. The degree of protonation of glutamate side chains should enable us to design a monocoordinated bipyridine metal complex, which is otherwise not possible since bipyridines normally form 1 : 3 complexes with Fe(II). Such a monocoordinated Fe(II)–bipyridine complex might display catalytic properties enabled by the availability of free coordination sites at the metal center.

The experiments below show that Fe(II) coordination to bipyridine can be directed towards the 1 : 1 complex by placing the bipyridine at the core of a peptide dendrimer bearing multiple anionic glutamate residues in the outer dendrimer branches at pH 6.5. Gradual removal of negative charge either by lowering the pH to 4.0 or by substituting neutral asparagine residues for the anionic glutamates leads to the stereoselective formation of 1 : 3 complexes, while complexation is substantially weakened when cationic residues are introduced. The metallopeptide dendrimer [Fe^{II}(**BP1**)] acts as a peroxidase enzyme model by catalyzing the oxidation of *o*-phenylenediamine with hydrogen peroxide with multiple turnover.

Results and discussion

Design and synthesis of bipyridine peptide dendrimers

Our first study of bipyridine containing peptide dendrimers used the building block 5-(fluorenylmethyloxycarbonyl)amino-5′-carboxy-2,2′-bipyridine for the synthesis of second generation peptide dendrimers with bipyridine in the focal point by solid phase peptide synthesis (SPPS). In order to create larger structures, we turned our attention to a convergent synthesis based on the thioether ligation, an approach which proved highly efficient for the assembly of protein-sized catalytic peptide dendrimers.[9b] In this process peptide dendrimers with a cysteine residue at their core are ligated by thioether

Table 1 Synthesis of bipyridine peptide dendrimers

Cpd	Sequence[a]	Yield/mg[b] (%)	MS calc./obs.
N1	$(AcES)_8(BEA)_4(BXY)_2BCD$	210 (24)	4297.1/4297.0
N2	$(AcQS)_8(BEA)_4(BXY)_2BCD$	44 (5)	4289.3/4289.0
N3	$(AcQS)_8(BQA)_4(BXY)_2BCD$	25 (3.6)	4285.4/4286.6
N4	$(AcKS)_8(BEA)_4(BXY)_2BCD$	92 (8.6)	4289.6/4289.0
BP1	$[(AcES)_8(BEA)_4(BXY)_2BC(SPy\text{-}D)]_2$	20.3 (49)	8774.5/8774.0
BP2	$[(AcQS)_8(BEA)_4(BXY)_2BC(SPy\text{-}D)]_2$	2.4 (6)	8758.7/8758.5
BP3	$[(AcQS)_8(BQA)_4(BXY)_2BC(SPy\text{-}D)]_2$	5.6 (16)	8750.9/8750.8
BP4	$[(AcKS)_8(BEA)_4(BXY)_2BC(SPy\text{-}D)]_2$	19.4 (28)	8759.4/8759.0

[a] X = 4-aminomethyl-benzoic acid, *B* = branching (*S*)-2,3-diaminopropionic acid, Py = 5-methyl-2-pyridyl, the C-terminus at D is $CONH_2$, see also Scheme 1. [b] Yields given for isolated material after preparative RP-HPLC, from SPPS for **N1–N4** and for the ligation reaction for **BP1–BP4**.

bond formation to four or eight chloroacetyl groups at the N-termini of another dendrimer. Similarly, we envisioned the double ligation of peptide dendrimer **N1** *via* its reactive core cysteine residue to 5,5′-bis(bromomethyl)-2,2′-bipyridine **1** to form the corresponding dendritic bipyridine **BP1** (Scheme 1). In this dendrimer the disubstituted bipyridine ligand would be buried within the peptide dendrimer core and would not "stick out" (as could occur with our previous bipy-dendrimers[12] or with linear peptides and proteins[15] all forming trimers), thus offering an optimal situation to control its metal coordination chemistry using the peptide dendrimer periphery. To this goal, the synthesis was also carried out with peptide dendrimers **N2–N4** in which the anionic glutamates in the G2 and G3 branches of **N1** were changed to neutral glutamines (**N2**, **N3**) or cationic lysine residues (**N4**).

The starting dendrimer **N1** and its analogs **N2–N4** were synthesized by SPPS as previously described.[11b] The bis(bromomethyl)-2,2′-bipyridine **1** was prepared adapting a literature procedure.[16] The dendrimers were then ligated to bipyridine **1** under an inert atmosphere in aqueous DMF using diisopropylethylamine as a base, which yielded the expected disubstituted bispyridine products **BP1–BP4** after acidification and purification by preparative reverse-phase HPLC (Table 1).

pH-dependent formation of Ni(II) and Fe(II) complexes

The aqueous metal complexation behavior of the bipyridine peptide dendrimer ligands **BP1–BP4** was characterized by spectrophotometric titration with Ni(II) (as $NiCl_2{\cdot}6H_2O$) and Fe(II) (as $Fe(NH_4)_2(SO_4)_2{\cdot}6H_2O$) following the shift of the π–π* absorption band of the bipyridyl moiety upon metal binding. The titrations were performed at pH 4.0 and pH 6.5 to study the effect of the ionization state of the carboxyl groups on metal binding.

In the case of Ni(II), which is known to bind two bipyridines as a square planar complex $[Ni(bipy)_2]^{2+}$ with a binding constant of 7×10^{13} M^{-2},[17] titrations gave clear isosbestic points and a 2 : 1 ligand : metal stoichiometry for all four ligands **BP1–BP4** at both pH 4.0 and pH 6.5 (Table 2, Fig. S16–S19†). The binding constants were all in the order of 10^{10} M^{-2}, which is comparable to that of the parent bipyridine complex.

Table 2 Complexation studies

		pH 4.0		pH 6.5	
Ligand	Metal	n[a]	$\beta_n \pm \sigma\beta_n$ (M^{-n})	n[a]	$\beta_n \pm \sigma\beta_n$ (M^{-n})
BP1	Ni^{2+}	2	$1.04 \pm 0.50 \times 10^{10}$	2	$1.01 \pm 0.76 \times 10^{10}$
BP2	Ni^{2+}	2	$2.2 \pm 1.0 \times 10^{11}$	2	$2.4 \pm 1.3 \times 10^{11}$
BP3	Ni^{2+}	2	$2.05 \pm 0.74 \times 10^{10}$	2	$5.9 \pm 3.5 \times 10^{10}$
BP4	Ni^{2+}	2	$1.05 \pm 0.30 \times 10^{9}$	2	$5.4 \pm 3.8 \times 10^{9}$
BP1	Fe^{2+}	3	$2.1 \pm 1.6 \times 10^{15}$	1	$2.11 \pm 0.73 \times 10^{5}$
BP2	Fe^{2+}	3	$8.2 \pm 2.4 \times 10^{13}$	[b]	n.d.
BP3	Fe^{2+}	3	$4.9 \pm 3.1 \times 10^{15}$	3	$8.1 \pm 3.2 \times 10^{14}$
BP4	Fe^{2+}	1[c]	Very low	1	$1.03 \pm 0.22 \times 10^{5}$
BP4–BP1 2 : 1[d]	Fe^{2+}	n.d.	n.d.	3	$1.06 \pm 0.60 \times 10^{15}$

[a] Ligand/metal binding stoichiometry determined from the UV-vis titration. [b] No isosbestic points observed: formation of at least two different complexes, fitting not possible. [c] Very weak binding. [d] Mixture of the peptide dendrimer ligands **BP4** and **BP1** at 2 : 1 molar ratio. n.d. = not determined.

The situation was much more differentiated with Fe(II), which normally binds three bipyridines to form a chiral octahedral complex $[Fe(bipy)_3]^{2+}$ with a binding constant of 3×10^{17} M^{-3}.[17] Complexes with one or two bipyridine ligands are normally not observed in solution because the third binding constant of 2,2′-bipyridine to Fe(II) is around five orders of magnitude higher than the first or second binding constants. Reported monobipyridine–Fe(II) complexes rely on steric hindrance of the metal center with large hydrophobic groups in order to prevent the formation of complexes with three bipyridine ligands and the few known examples of monobipyridine–iron(II) complexes are reported to be rather unstable[18] or to readily react with nucleophiles such as water, acetonitrile and pyridine.[19] In our case the charges in the dendrimer prevent the complexation with a second bipy ligand and stable monobipy complexes are formed in aqueous media. Thus, the complexation ability of Fe(II) by the dendritic bipyridines **BP1–BP4** was dependent not only on the ligand but also on the pH value (Table 2).

Ligand **BP1**, which carries 24 glutamate residues in the outer dendrimer branches, formed the expected 1 : 3 complex $[Fe^{II}(\mathbf{BP1})_3]$ with a binding constant of 2.1×10^{15} M^{-3} at the acidic value of pH 4.0. Formation of the 1 : 3 metal–ligand complex was evidenced by formation of a pink solution and by the appearance of the characteristic metal-to-ligand charge transfer (MLCT) band in the visible region (λ_{max} = 534 nm).

At pH 4.0, the majority of the 24 glutamate side chains of **BP1** are expected to be in the uncharged, protonated state. At pH 6.5, by contrast, titration of **BP1** with Fe(II) indicated the formation of a 1 : 1 complex $[Fe^{II}(\mathbf{BP1})]$ with a binding constant of 2.1×10^5 M^{-1} (Fig. 2). The absence of the 1 : 3 complex was also indicated by the fact that the solution remained colorless, and by the absence of the characteristic MLCT band. At pH 6.5 the 24 glutamate side chains in **BP1** are expected to be largely in the anionic, deprotonated state. Repulsion between like charges in the dendritic branches of **BP1** probably prevents the formation of the 1 : 3 complex of Fe(II) with the bipyridine groups at the dendrimer core by overriding its normally

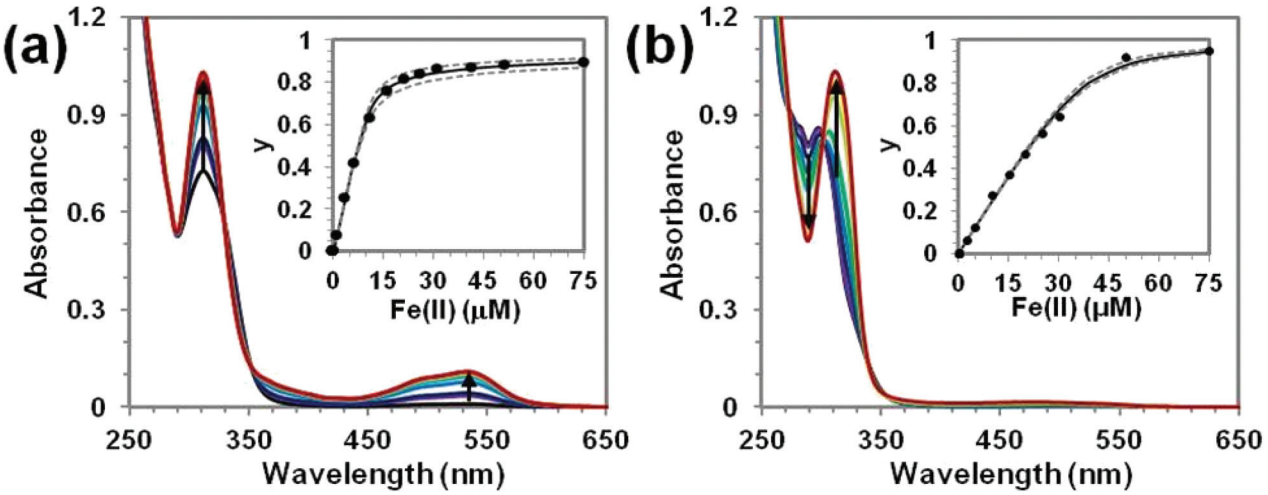

Fig. 2 Spectrophotometric titrations of **BP1**, 50 μM, with Fe(II) in AcONa buffer, pH 4.0 (a) and in HEPES buffer, pH 6.5 (b). Insets with fitting of the normalized titration curves. y ($y = (A - A_0)/(A_\infty - A_0)$) is the fraction of a metal bound ligand, the dotted lines represent the confidence interval for the calculated titration curves (solid lines).

observed binding cooperativity. The coordination sphere can then be saturated by iron complexation with amino acid side chains, such as carboxylates from glutamate residues, and/or water molecules. The formation of the 1 : 1 rather than 1 : 3 Fe^{II}–**BP1** complex at pH 6.5 was apparently due to thermodynamic rather than kinetic factors, as evidenced by the disappearance of the MLCT band characteristic of the 1 : 3 complex upon raising the pH of a solution of [Fe^{II}(**BP1**)$_3$] from pH 3.5 to pH 6.5, and its reappearance upon reacidification of the same solution (Fig. S24†). The protonation state of **BP1** was further investigated by a pH titration in the absence and in the presence of Fe(II) (Fig. S25†). The apparent pK_a showed a shift to higher values in the presence of Fe(II), suggesting that protonation of glutamate side chains in the dendrimer **BP1** is modulated by metal complexation.

A somewhat similar situation was observed with ligand **BP2**, which has the same structure as **BP1**, except that 16 of the 24 glutamate residues present in the G3 branches have been mutated to glutamine residues with a polar but non-ionizable carboxamide side chain, while 8 ionizable glutamates are retained in the G2 branches. Ligand **BP2** formed the [Fe^{II}(**BP2**)$_3$] complex at pH 4.0 with a binding constant of 8.2×10^{13} M^{-3}. However titration of **BP2** with Fe(II) at pH 6.5 did not give an isosbestic point and the characteristic MLCT band of the 1 : 3 complex was not visible (Fig. S20†). This suggests that binding of Fe(II) to **BP2** at pH 6.5 results in the formation of a mixture of products and shows that the negative charges accumulating in **BP2** at pH 6.5 by deprotonation of the eight ionizable glutamate side chains in the G2 branches of **BP2** are also capable of perturbing coordination of the core bipyridine ligand to Fe(II) as observed in **BP1**.

The effect of the glutamate side chain ionization on the coordination properties of **BP1** and **BP2** with Fe(II) at pH 6.5 was confirmed by the observation that ligand **BP3**, in which all 24 glutamates of **BP1** have been mutated to non-ionizable, neutral glutamine residues, formed the expected 1 : 3 complex [Fe^{II}(**BP3**)$_3$] at both pH values, with binding constants 5×10^{15} M^{-3} at pH 4.0 and 8×10^{14} M^{-3} at pH 6.5 (Fig. S21†). The coordination chemistry of the bipyridine ligand at the dendrimer core with Fe(II) was also affected by the presence of multiple positive charges in the form of the 16 positively charged lysine side chains in dendrimer **BP4**. At pH 6.5, where these positive charges are partly compensated by the presence of eight anionic glutamate side chains in the G2 branches, Fe(II) formed the 1 : 1 complex [Fe^{II}(**BP4**)] as observed with **BP1** at that pH value. At pH 4.0 however, under which conditions the eight glutamate side chains are expected to occur as uncharged carboxylic acids and ligand **BP4** carries a much larger net positive charge, Fe(II) binding was almost completely inhibited, with only weak binding consistent with formation of the 1 : 1 complex [Fe^{II}(**BP4**)] (Fig. S22†).

While both **BP1** and **BP4** formed 1 : 1 complexes with Fe(II) at pH 6.5, titration of a 1 : 2 mixture of **BP1** and **BP4** resulted in the formation of the 1 : 3 complex [Fe^{II}(**BP4**)$_2$(**BP1**)] (binding constant 1.1×10^{15} M^{-3}) with its characteristic pink color and an MLCT band as observed for the titration with the glutamine containing ligand **BP3**. Complex [Fe^{II}(**BP4**)$_2$(**BP1**)] was apparently a single species as evidenced by HPLC analysis (Fig. S27†). This showed that **BP1** and **BP4** were indeed capable of forming a 1 : 3 complex with Fe(II), and confirmed that formation of the 1 : 1 complexes observed in the Fe(II) titrations with the pure ligands was caused by repulsion among like charges in the dendrimer branches.

The fact that the square planar nickel complex with two ligands is unaffected by pH compared to the octahedral iron complex with three dendritic ligands is likely due to the higher accumulation of negative charges at basic pH in the Fe(II) complex and by the preferred complex geometries. The three dendritic moieties around the Fe(II) are closer to each other than the two dendrimers around the Ni(II). Therefore the 2 : 1

coordination and the square planar geometry are less sensitive to the charge accumulation effects compared to the 3 : 1 coordination with octahedral geometry.

NMR and CD experiments

Further characterization of the ligands and their Fe(II) complexes was obtained by ^{1}H NMR and CD spectroscopy. Diffusion coefficients obtained by ^{1}H NMR diffusion experiments at pH 4.0 and pH 6.5 revealed an increase in size for the polyglutamate containing ligand **BP1**, no change for the glutamine containing ligand **BP3**, and a decrease in size for ligand **BP4** (Table 3). The pH dependent size variations for **BP1** and **BP4** correlate well with the deprotonation of the glutamic acid side chains inducing an increase in the number of negative charges for **BP1**, and a partial neutralization of the positive charges of the lysine side chains for **BP4**.

The complexes [Fe^{II}(**BP1**)$_3$] at pH 4.0 and [Fe^{II}(**BP3**)$_3$] at both pH 4.0 and 6.5 gave ^{1}H NMR spectra with sharp peaks indicative of the low spin state of the Fe(II) in the three fold coordinated complexes, in agreement with the spectrophotometric titrations. Formation of these 1 : 3 complexes only induced a small increase in the hydrodynamic radii compared to the free ligands in spite of the change in molecular mass from ~8800 to 25 000, probably due to a more compact space-filling arrangement of the ligands within the metal complexes compared to the free dendrimers. Most likely the free ligands do not have the same shape and rigidity as their 3 : 1 Fe(II) complexes: the latter are roughly spherical and quite rigid due to the octahedral symmetry of the bipyridyl cores around the metal center, while the former have two roughly conical domains hinging on a small, rigid core. The dendrimers' radii at different pH values are better comparable because the dendrimer shape should be similar.[20] No NMR data could be acquired for the high-spin monocoordinated complexes [Fe^{II}(**BP1**)] and [Fe^{II}(**BP4**)]. The mixed complex [Fe^{II}(**BP4**)$_2$(**BP1**)] at pH 6.5 had a size comparable to that of the mixture of the ligands before addition of Fe(II), suggesting a pre-aggregation of the ligands directed by electrostatic interactions before complexation.

Table 3 Hydrodynamic radii of the dendrimer ligands and of their 3 : 1 Fe(II) complexes

Compound	c (mM)	pH[a]	Eq Fe(II)	$D \pm \sigma D$[b] (10^{-10} m^2 s^{-1})	$r_h \pm \sigma r_h$[c] (nm)
BP1	0.90	4.0	—	1.19 ± 0.030	1.71 ± 0.04
BP1	0.85	6.5	—	0.94 ± 0.035	2.14 ± 0.06
BP3	0.27	4.0	—	1.23 ± 0.032	1.66 ± 0.04
BP3	0.27	6.5	—	1.21 ± 0.078	1.7 ± 0.1
BP4	0.85	4.0	—	1.10 ± 0.024	1.84 ± 0.04
BP4	0.85	6.5	—	1.15 ± 0.034	1.76 ± 0.05
[Fe^{II}(**BP1**)$_3$]	0.90	4.0	0.30	0.91 ± 0.029	2.23 ± 0.07
[Fe^{II}(**BP3**)$_3$]	0.27	4.0	0.28	1.00 ± 0.11	2.0 ± 0.2
[Fe^{II}(**BP3**)$_3$]	0.27	6.5	0.28	1.08 ± 0.10	1.9 ± 0.2
2**BP4** + **BP1**	0.65	6.5	—	0.87 ± 0.032	2.34 ± 0.09
[Fe^{II}(**BP4**)$_2$(**BP1**)]	0.66	6.5	0.29	0.85 ± 0.024	2.40 ± 0.07

[a] pH values were adjusted by addition of 0.1–0.3 M NaOD. [b] Diffusion coefficients obtained by NMR diffusion experiments in D_2O at 30 °C. [c] Hydrodynamic radii were calculated from the diffusion coefficients using the Stokes–Einstein relationship $r_h = k_B T/(6\pi\eta D)$.

CD spectra of the 1 : 3 complexes [Fe^{II}(**BP1**)$_3$], [Fe^{II}(**BP3**)$_3$] and [Fe^{II}(**BP4**)$_2$(**BP1**)] showed intense signals at 275–350 nm (bipy π–π* band) and at 450–600 nm (MLCT band), with a Cotton effect pattern which indicates a strong prevalence of the Δ-isomer at the metal center (Fig. 3, Table 4). While preference for the Δ-isomer over the Λ-isomer has been reported with other Fe(II) complexes of bipyridine-derived peptide ligands made of all L residues,[21] the Cotton effect was particularly strong with the complexes [Fe^{II}(**BP1**)$_3$] and [Fe^{II}(**BP4**)$_2$-(**BP1**)], suggesting that the Δ-isomer formed almost exclusively.

Peroxidase activity of [Fe^{II}(BP1)]

As a model for a metalloenzyme catalyzed reaction we focused on the oxidation of chromogenic substrates by hydrogen peroxide, a reaction compatible with aqueous conditions and

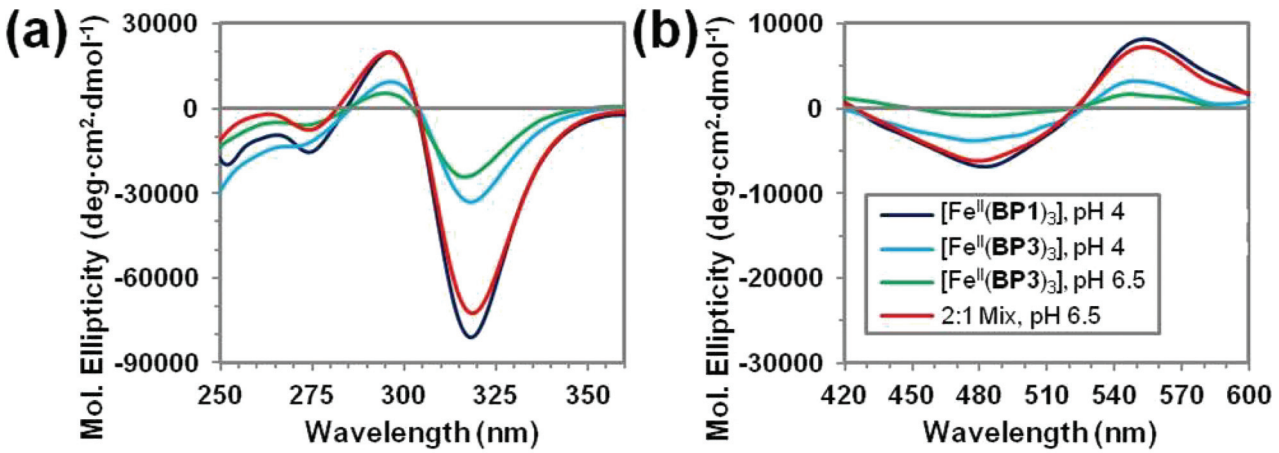

Fig. 3 CD spectra of the 3 : 1 Fe(II) complexes of the dendrimer ligands in the spectral regions of (a) the bipyridyl chromophore (λ_{max} ≈ 310 nm) and of (b) the MLCT chromophore (λ_{max} ≈ 530 nm). Ligands: **BP1**, 50 μM in AcONa buffer, pH 4.0; **BP3**, 50 μM in AcONa buffer, pH 4.0; **BP3**, 50 μM in HEPES buffer, pH 6.5; 2 : 1 mixture of **BP4** and **BP1**, total concentration 50 μM in HEPES buffer, pH 6.5.

Table 4 Molar ellipticities of Fe(II) dendrimer complexes[a]

		MLCT band		bipy π–π* band	
BPn[b]	pH	Cotton+[c] (λ_M, [Θ_T])[d]	Cotton−[c] (λ_M, [Θ_T])[d]	Cotton+[c] (λ_M, [Θ_T])[d]	Cotton−[c] (λ_M, [Θ_T])[d]
BP1	4.0	555, 8600	484, −7100	296, 20 000	318, −82 000
BP3	4.0	544, 3300	477, −3900	296, 9500	317, −33 000
BP3	6.5	562, 1400	486, −940	295, 7400	317, −13 000
BP4–BP1 2 : 1 Mix[e]	6.5	557, 7700	479, −6400	296, 20 200	319, −74 000

[a] CD measurements were performed at 25 °C. [b] Peptide dendrimer ligand forming a 3 : 1 Fe(II) complex. [c] Data refer to the positive (Cotton+) and negative (Cotton−) maxima for each of the two bands. [d] Maximum wavelengths (λ_M) are expressed in nanometre, and total molar ellipticities [Θ_T] are expressed in deg cm^2 dmol^{-1}. [e] Refers to the complex [Fe^{II}(**BP4**)$_2$(**BP1**)].

Table 5 Catalytic parameters for the oxidation of OPD by H_2O_2 with Fe(II) catalysts[a]

Catalyst (4.8 μM)	Conversion at 4 h[b] (μM)	$TON_{4\ h}$[c]	$TOF_{1\ h}$[d] (h^{-1})
$Fe^{2+}_{(aq)}$	2.6 ± 0.9	0.5 ± 0.2	0.25 ± 0.06
$[Fe(bipy)_3]^{2+}$	12.0 ± 0.9	2.5 ± 0.2	0.72 ± 0.04
[Fe^{II}(**BP1**)][e]	171 ± 13	36 ± 3	16.1 ± 0.8

[a] Experiments were performed in duplicate. Conditions: 1.9 mM substrate (OPD), 3.8 mM H_2O_2, pH 6.5 (12 mM HEPES buffer), 25 °C. [b] The background value for the reaction in the absence of Fe(II) is 5.0 ± 0.6 μM. Values for the experiments with Fe^{II} catalysts are background subtracted. [c] Turnover number (mol oxidized substrate/mol catalyst) at the time given. Amounts of the oxidized substrate are background subtracted. [d] Turnover frequency (mol oxidized substrate/(mol catalyst × time)) at the time given. Amounts of the oxidized substrate are background subtracted. [e] Results of [Fe^{II}(**BP1**)] are the average of two independent experiments, each performed in duplicate.

microtiter plate experiments. The reaction can be catalyzed by peroxidases such as horseradish peroxidase and serves as a reporter system in various enzyme assays and immunoassays. In horseradish peroxidase a porphyrin bound Fe(III) forms a highly oxidized species (Fe(IV) or Fe(V) porphyrin) which then oxidizes the dye precursor. Similar oxidation reactions take place with various Fe(II) complexes (Fenton reaction)[22,23] including Fe(II) bipyridines. Although the mechanism of these reactions remains poorly understood, we hypothesized that the availability of free coordination sites in the mono-bipyridine complex [Fe^{II}(**BP1**)] might favor peroxidase activity by allowing direct coordination of H_2O_2 and possibly of the substrate to the metal center. Indeed in this complex four out of six coordination sites of the metal are occupied by monodentate ligands (water and/or carboxyl groups from the peptide dendrimer) and available for rapid exchange with external ligands.

The possible peroxidase reactivity of [Fe^{II}(**BP1**)] was investigated by screening the oxidation of chromogenic dyes by hydrogen peroxide in the presence or absence of the metal complex, using aqueous Fe^{2+} and $[Fe(bipy)_3]^{2+}$ as controls for the background activity of Fe(II). The aniline dye precursors 3,3′-diaminobenzidine (DAB) and *o*-phenylenediamine (OPD) reacted within minutes in the presence of the metallodendrimer [Fe^{II}(**BP1**)], while almost no reaction took place with Fe^{2+} or $[Fe(bipy)_3]^{2+}$ under the same conditions. The reaction was investigated in detail with *o*-phenylenediamine (OPD) because the colorimetric signal obtained was more stable (Table 5). While the reactions with Fe^{2+} and $[Fe(bipy)_3]^{2+}$ were very slow and stopped after one or two catalyst turnover, the reaction with [Fe^{II}(**BP1**)] was catalytic with multiple turnover.[24] Catalysis with [Fe^{II}(**BP1**)] followed Michaelis–Menten kinetics with constants k_{cat} of 1.0 ± 0.1 min^{-1} (k_{cat}/k_{uncat} = 90 000) and K_M = 1.50 ± 0.2 mM (Fig. 4).

The catalytic reaction of [Fe^{II}(**BP1**)] implies that the Fe(III) produced in the oxidation step is reduced back to Fe(II) in the catalytic cycle, while this is apparently not the case with the controls Fe^{2+} and $[Fe(bipy)_3]^{2+}$ (Scheme 2). The special mono-coordinated bipyridine complex probably conveniently modulates the redox potential of the Fe(III)/Fe(II) couple (the corresponding standard redox potentials for the $Fe^{3+}_{(aq)}/Fe^{2+}_{(aq)}$ and $[Fe(bipy)_3]^{3+}/[Fe(bipy)_3]^{2+}$ are reported to be +771 mV and +960 mV respectively)[25] to allow both for Fe(II) oxidation by H_2O_2 and for Fe(III) recycling.

The increased activity of modified bipyridine is not trivial. In a reported peroxidase model, introduction of four peptides on pentadentate ligands with four pyridine rings gave a penta-coordinated Fe(II) complex. In contrast to our results, the peptide moieties reduced the activity of the Fe(II) as a catalyst for the hydrogen peroxide oxidation of ABTS compared to the complex without peptides appended to pyridines.[26]

Conclusion

The experiments above show that the polyanionic peptide dendrimer **BP1** forms a 1 : 1 Fe(II) complex featuring a mono-bipyridine coordination. Control of bipyridine coordination to Fe(II) in dendrimer **BP1** occurs by means of the multiple electrostatic charges of the glutamate residues present in the G2 and G3 branches, as evidenced by the fact that the complex is formed specifically at pH 6.5, where the side chains are mostly anionic, while the standard 1 : 3 complex [Fe^{II}(**BP1**)$_3$] is formed (mainly as the Δ-stereoisomer) at pH 4.0, where the side chains are mostly in the protonated neutral state. Further evidence for the control of coordination was also provided by the dendrimer analogs **BP2–BP3**, bearing a smaller amount of negative charge in their branches, as well as by the dendrimer analog **BP4**, bearing a net positive charge.

The metallopeptide dendrimer [Fe^{II}(**BP1**)] acts as a peroxidase enzyme model by catalyzing the oxidation of *o*-phenylenediamine with hydrogen peroxide with multiple turnover and

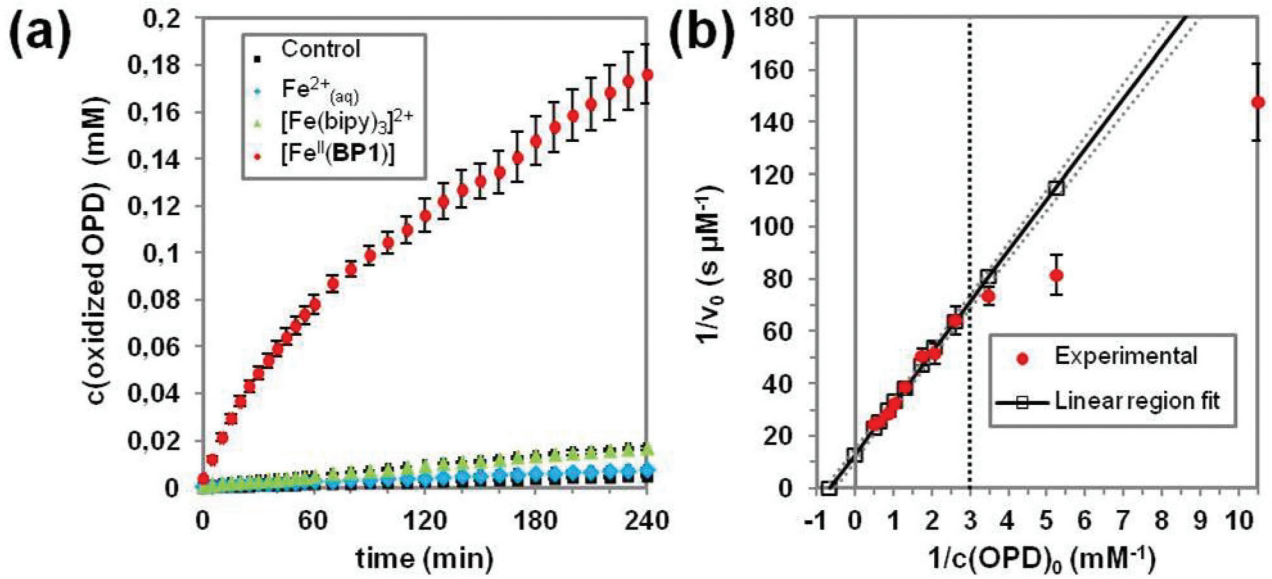

Fig. 4 (a) Oxidation of the activated aromatic substrate OPD by H_2O_2 in the presence of different Fe(II) sources and control experiment in the absence of Fe(II) sources. Conditions: substrate 1.9 mM, H_2O_2 3.8 mM, Fe(II) sources 4.8 μM, in 12 mM aqueous HEPES buffer, pH 6.5, at 25 °C. (b) Double reciprocal plot for OPD oxidation by H_2O_2 in the presence of [Fe^{II}(**BP1**)]. Conditions: substrate 0.095–1.9 mM, H_2O_2 3.8 mM, catalyst 4.8 μM, in 12 mM aqueous HEPES buffer, pH 6.5, at 25 °C. The black vertical dotted line delimits the linear portion of the graph. The two grey dotted curves represent the confidence interval for the fitting. Both experiments were followed using a 96-well microplate reader (λ = 425 nm). Absorbance was converted into concentration of the oxidized substrate using a calibration curve, which was linear in the observed absorbance range. Data for the reaction in the presence of [Fe^{II}(**BP1**)] are the average of two independent experiments, each performed in duplicate.

k_{cat}/k_{uncat} = 90 000, while aqueous Fe^{2+} or its bipyridine complex $[Fe(bipy)_3]^{2+}$ are themselves much less active as catalysts. This represents the first example of aqueous catalysis by a metallopeptide dendrimer.

It should be noted that the possibility to modulate the coordination of bipyridine between tri-coordination or mono-coordination within a narrow pH range (4.0–6.5) by embedding it within a peptide dendrimer structure has not been described before. Small molecule catalysts lack the ability to modulate the coordination sphere of metal ions by changing the pH and their coordination numbers are normally adjusted with the proper ligands or by steric congestion. In that sense flexible branched nanostructures such as the bipyridine peptide dendrimers described here can be seen as attractive structures as mimics of metalloenzymes.

Experimental section

Synthesis of bipyridine peptide dendrimers

Cysteine-containing peptide dendrimers (**N1**, **N2**, **N3**, **N4**) were synthesized on solid-phase employing the Fmoc/*t*Bu strategy and purified by RP-HPLC. Experimental conditions and characterization are described in the ESI.†

BP1. 5,5′-Bis(bromomethyl)-2,2′-bipyridine (**1**, 1.7 mg, 4.8 μmol) and diisopropylethyl amine (DIEA, 25 μL, 150 μmol) were dissolved in 0.4 mL DMF under Ar. The resulting solution was added to **N1** (43.3 mg, 10 μmol) in 0.5 mL milliQ H_2O under Ar. A suspension resulted, which gradually turned to a clear solution. After 2 h the reaction mixture was quenched by addition of TFA (20 μL, 200 μmol), the mixture was diluted with 10 mL H_2O and lyophilized. The crude product was redissolved in 10 mL H_2O and purified by preparative HPLC to yield 20.3 mg (2.3 μmol, 49%) of the title compound as TFA salt. MS (ESI−) calcd for $C_{360}H_{502}N_{92}O_{162}S_2$: *m*/*z* 8774.5, found 8774.0 ([M − H]$^-$).

BP2. The reaction of **1** (0.84 mg, 2.3 μmol) and **N2** (22.3 mg, 4.7 μmol) yielded 2.4 mg (0.25 μmol, 6.6%) of the title compound as TFA salt. MS (ESI−) calcd for $C_{360}H_{518}N_{108}O_{146}S_2$: *m*/*z* 8758.7, found 8758.9 ([M]$^-$).

BP3. The reaction of **1** (1.34 mg, 3.7 μmol) and **N3** (34.5 mg, 7.6 μmol) yielded 5.6 mg (0.58 μmol, 17%) of the title compound as TFA salt. MS (MALDI) calcd for $C_{360}H_{526}N_{116}O_{138}S_2$: *m*/*z* 8750.9, found 8750.9 ([M]$^+$).

BP4. The reaction of **1** (2.31 mg, 6.4 μmol) and **N4** (77.1 mg, 13.3 μmol) according to the protocol above yielded 19.4 mg (1.77 μmol, 28%) of the title compound as TFA salt. MS (MALDI) calcd for $C_{376}H_{582}N_{108}O_{130}S_2$: *m*/*z* 8759.4, found 8761.2 ([M + H]$^+$).

General procedure for spectrophotometric titrations

1–2 mg of the lyophilized dendrimers were dissolved in degassed milliQ H_2O to obtain solutions at concentrations around 1 mM. Just before the titrations, aliquots of the stock solutions were diluted in the appropriate buffer (AcONa 20 mM, pH 4.0, or HEPES 20 mM, pH 6.5) to a concentration of 25–50 μM and 1.00 mL of the diluted solutions were transferred into reduced volume 1.00 cm optical path quartz cells. The metal salts ($NiCl_2{\cdot}6H_2O$ or $Fe(NH_4)_2(SO_4)_2{\cdot}6H_2O$) were

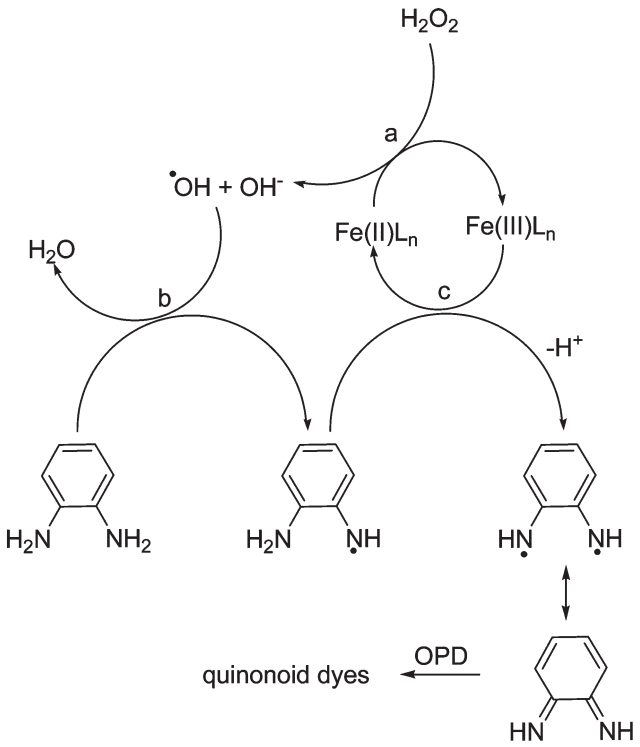

Scheme 2 Proposed pathway for the catalytic oxidation of the activated aromatic substrate *ortho*-phenylenediamine (OPD) into quinonoid dyes. Hydrogen peroxide oxidizes Fe(II) in a Fenton-like reaction (a) generating an hydroxyl radical, which abstracts one hydrogen atom from the substrate (b), forming H_2O and a semiquinonoid radical. The latter is able to reduce back the oxidized Fe(III) (c) giving an *o*-quinonimine moiety, which reacts further with OPD forming quinonoid dyes.

dissolved in milliQ H_2O to prepare 1–3 mM solutions. The cell temperature was thermostated at 25.0 °C. For each experimental point, increasing amounts of the metal solutions were added to the UV-cells with a syringe, the solutions were mixed thoroughly and allowed to stand until the equilibrium was reached (after 50 min for Ni(II) or 60 min for Fe(II), as found in preliminary tests) before the spectrum was acquired. Addition of metal solutions continued until no further changes were observed in the spectra. In the case of experiments involving Fe(II), all solutions were prepared under argon and septum stoppered UV cells were employed.

Circular dichroic (CD) measurements

Freshly prepared solutions of 3 : 1 bipyridine peptide dendrimer–Fe(II) complexes (identified by the presence of the characteristic MLCT visible band in the corresponding spectrophotometric titration) 25–50 μM in the appropriate buffer (AcONa buffer, pH 4.0, or HEPES buffer, pH 6.5) were tested, as well as 50 μM solutions of **BP1** in both buffers and of the 1 : 1 **BP1**–Fe(II) complex in HEPES buffer. The two buffers were used as blanks.

Instrumental parameters: $250 \leq \lambda/\text{nm} \leq 600$, scan speed 100 nm min^{-1}, step 0.5 nm, band width 1.0 nm, response 1.0 s. Reduced volume 1.0 cm optical path quartz cells thermostated at 25.0 °C were employed. 6–8 scans were recorded and averaged for each sample. After subtraction of the appropriate blank, circular dichroic signals (ΔA) were converted into total molar ellipticities ($[\Theta_T]$) and the spectra were smoothed.

Catalysis experiment

4.0 mM solution of OPD and 1.0 mM, 0.4 mM diluted solutions were prepared in HEPES buffer, pH 6.5 (full details of the experiment in the ESI†). A 100 μM solution of Fe(II) source ($Fe(NH_4)_2(SO_4)_2 \cdot 6H_2O$ or one of the complexes) was prepared. The required amounts of the three substrate solutions and of HEPES buffer were pipetted into the wells of a microtiter plate so that one control row and two sample rows of 12 wells each with 0–200 nmol OPD in 65 (control row) or 60 (sample rows) μL solution were obtained. 40 μL 10 mM H_2O_2 (freshly prepared by dilution of 30% H_2O_2 with milliQ H_2O) were added to each well and the plate was mixed thoroughly. 5 μL of 100 μM Fe(II) source solution were rapidly added to the two sample rows and the plate was mixed thoroughly. The plate was then kept at 25.0 °C and shaken gently during 4 h, with readings at λ 425 nm every minute.

Acknowledgements

This work was supported financially by the University of Berne, the Swiss National Science Foundation, and the European Union FP7-ITN-238434.

References

1 (*a*) G. R. Newkome, C. N. Moorefield and F. Vögtle, *Dendritic Molecules: Concepts, Synthesis, Applications*, VCH, Weinheim, 2001; (*b*) *Dendrimers IV: Metal Coordination, Self Assembly and Catalysis, Topics in Current Chemistry*, ed F. Vögtle and C. A. Schalley, Springer-Verlag, Berlin, 2001, vol. 217; (*c*) C. C. Lee, J. A. MacKay, J. M. J. Fréchet and F. C. Szoka, *Nat. Biotechnol.*, 2005, **23**, 1517–1526; (*d*) D. Astruc, E. Boisselier and C. Ornelas, *Chem. Rev.*, 2010, **110**, 1857–1959.
2 (*a*) B. Helms and J. M. J. Fréchet, *Adv. Synth. Catal.*, 2006, **348**, 1125–1148; (*b*) J. Kofoed and J.-L. Reymond, *Curr. Opin. Chem. Biol.*, 2005, **9**, 656–664.
3 R. Breinbauer and E. N. Jacobsen, *Angew. Chem., Int. Ed.*, 2000, **39**, 3604–3607.
4 G. Zaupa, P. Scrimin and L. J. Prins, *J. Am. Chem. Soc.*, 2008, **130**, 5699–5709.
5 Review on catalytic dendrimers: D. Astruc and F. Chardac, *Chem. Rev.*, 2001, **101**, 2991–3023.
6 (*a*) A. Esposito, E. Delort, D. Lagnoux, F. Djojo and J.-L. Reymond, *Angew. Chem., Int. Ed.*, 2003, **42**, 1381–1383; (*b*) T. Darbre and J.-L. Reymond, *Acc. Chem. Res.*, 2006, **39**, 925–934; (*c*) T. Darbre and J.-L. Reymond, *Org. Biomol. Chem.*, 2012, **10**, 1483–1492.

7 (*a*) E. Delort, T. Darbre and J.-L. Reymond, *J. Am. Chem. Soc.*, 2004, **126**, 15642–15643; (*b*) E. Delort, N.-Q. Nguyen-Trung, T. Darbre and J.-L. Reymond, *J. Org. Chem.*, 2006, **71**, 4468–4480; (*c*) R. Biswas, N. Maillard, J. Kofoed and J.-L. Reymond, *Chem. Commun.*, 2010, 8746–8748.

8 (*a*) S. Javor, E. Delort, T. Darbre and J.-L. Reymond, *J. Am. Chem. Soc.*, 2007, **129**, 13238–13246; (*b*) N. Maillard, T. Darbre and J.-L. Reymond, *J. Comb. Chem.*, 2009, **11**, 667–675; (*c*) N. Maillard, R. Biswas, T. Darbre and J.-L. Reymond, *ACS Comb. Sci.*, 2011, **13**, 310–320.

9 (*a*) J. Kofoed, T. Darbre and J.-L. Reymond, *Org. Biomol. Chem.*, 2006, **4**, 3268–3281; (*b*) N. A. Uhlich, T. Darbre and J.-L. Reymond, *Org. Biomol. Chem.*, 2011, **9**, 7071–7084.

10 A. Clouet, T. Darbre and J.-L. Reymond, *Angew. Chem., Int. Ed.*, 2004, **43**, 4612–4615.

11 (*a*) P. Sommer, N. A. Uhlich, J.-L. Reymond and T. Darbre, *ChemBioChem*, 2008, **9**, 689–693; (*b*) N. A. Uhlich, A. Natalello, R. U. Kadam, S. M. Doglia, J.-L. Reymond and T. Darbre, *ChemBioChem*, 2010, **11**, 358–365.

12 N. A. Uhlich, P. Sommer, C. Bühr, S. Schürch, J.-L. Reymond and T. Darbre, *Chem. Commun.*, 2009, 6237–6239.

13 (*a*) C. Kaes, A. Katz and M. W. Hosseini, *Chem. Rev.*, 2000, **100**, 3553–3590; (*b*) U. S. Schubert and C. Eschbaumer, *Angew. Chem., Int. Ed.*, 2002, **41**, 2892–2926.

14 Examples of dendritic bipyridine ligands: (*a*) J. Issberner, F. Vogtle, L. De Cola and V. Balzani, *Chem.–Eur. J.*, 1997, **3**, 706–712; (*b*) G. R. Newkome, E. He and C. N. Moorefield, *Chem. Rev.*, 1999, **99**, 1689–1746.

15 (*a*) M. R. Ghadiri and C. Choi, *J. Am. Chem. Soc.*, 1990, **112**, 1630–1632; (*b*) M. R. Ghadiri, C. Soares and C. Choi, *J. Am. Chem. Soc.*, 1992, **114**, 4000–4002; (*c*) M. Lieberman and T. Sasaki, *J. Am. Chem. Soc.*, 1991, **113**, 1470–1471; (*d*) M. Lieberman, M. Tabet and T. Sasaki, *J. Am. Chem. Soc.*, 1994, **116**, 5035–5044; (*e*) M. W. Mutz, G. L. McLendon, J. F. Wishart, E. R. Gaillard and A. F. Corin, *Proc. Natl. Acad. Sci. U. S. A.*, 1996, **93**, 9521–9526; (*f*) M. Gochin, R. K. Guy and M. Case, *Angew. Chem., Int. Ed.*, 2003, **42**, 5325–5328; (*g*) H. Ishida, Y. Maruyama, M. Kyakuno, Y. Kodera, T. Maeda and S. Oishi, *ChemBioChem*, 2006, **7**, 1567–1570; (*h*) D. E. Przybyla and J. Chmielewski, *J. Am. Chem. Soc.*, 2008, **130**, 12610–12611; (*i*) M. M. Pires, D. E. Przybyla and J. Chmielewski, *Angew. Chem., Int. Ed.*, 2009, **48**, 7813–7817; (*j*) R. J. Radford and F. A. Trezcan, *J. Am. Chem. Soc.*, 2009, **131**, 9136–9137; (*k*) H. K. Munch, S. T. Heide, N. J. Christensen, T. Hoeg-jensen, P. W. Thulstrup and K. J. Jensen, *Chem.–Eur. J.*, 2011, **17**, 7198–7204.

16 B. Imperiali, T. J. Prins and S. L. Fisher, *J. Org. Chem.*, 1993, **58**, 1613–1616.

17 (*a*) H. Irving and D. H. Mellor, *J. Chem. Soc.*, 1962, 5222–5237; (*b*) T. Sasaki and M. Lieberman, *Tetrahedron*, 1993, **49**, 3677–3689; (*c*) K. A. Connors, *Binding Constants – The Measurement of Molecular Complex Stability*, John Wiley and Sons, 1987, pp. 21–102, 141–167.

18 The complex $[Fe^{II}(pb)_2\text{–}(CH_3CN)_2]$ (pb = (−)4,5-pinene-2,2-bipyridine) was reported to be moderately stable ($t_{1/2}$ = 2 h) and to decompose to the trimer, Y. Mekmouche, H. Hummel, R. Y. N. Ho, L. Que Jr., V. Schünemann, F. Thomas, A. X. Trautwein, C. Lebrun, K. Gorgy, J.-C. Leprêtre, M.-N. Collomb, A. Deronzier, M. Fontecave and S. Ménage, *Chem.–Eur. J.*, 2002, **8**, 1196–1204.

19 Complex of Fe(II) with 6,6′-(2,4,6-triisopropylphenyl)-2,2′-bipyridine ($FeCl_2$tripbipy) was prepared in toluene. The ligand with large and rigid groups and a narrow coordination region between them enforced a tetrahedral geometry. E. E. Benson, A. L. Rheingold and C. P. Kubiak, *Inorg. Chem.*, 2012, **49**, 1458–1464.

20 The Stokes–Einstein equation ($r_h = k_BT/6\pi\eta D$) relates the diffusion coefficient of a particle with its hydrodynamic radius. The relationship between the hydrodynamic radii and the characteristic dimensions (*e.g.* radius for a spherical particle, main axes for a tubular particle and so on) of the real particles depends on several factors, among which the most important ones are the shape and flexibility of the particles. Therefore comparisons are better made among compounds with similar shapes.

21 (*a*) D.-R. Ahn, T. W. Kim and J.-I. Hong, *J. Org. Chem.*, 2001, **66**, 5008–5011; (*b*) S. J. Milder, J. S. Gold and D. S. Kliger, *J. Am. Chem. Soc.*, 1986, **108**, 8295–8296; (*c*) S. G. Telfer, G. Bernardinelli and A. F. Williams, *Dalton Trans.*, 2003, 435–440; (*d*) S. G. Telfer, X.-J. Yang and A. F. Williams, *Dalton Trans.*, 2004, 699–705.

22 H. J. H. Fenton, *J. Chem. Soc.*, 1894, **65**, 899–910.

23 (*a*) F. Buda, B. Ensing, M. C. M. Gribnau and E. J. Baerends, *Chem.–Eur. J.*, 2003, **9**, 3436–3444; (*b*) P. A. MacFaul, D. D. M. Wayner and K. U. Ingold, *Acc. Chem. Res.*, 1998, **31**, 159–162; (*c*) D. T. Sawyer, A. Sobkowiak and T. Matsushita, *Acc. Chem. Res.*, 1996, **29**, 409–416.

24 It is possible that the sulfide groups in the ligand are also oxidized by H_2O_2. We have done two controls to check for oxidation of the sulfide bond in the ligand. After treating [Fe(**BP1**)] with 4 mM H_2O_2 in the absence of OPD, the complex had the same retention time by HPLC as the complex in buffer (see Fig. S38†). As a second control Fmoc-methionine was treated with $[Fe(bipy)_3]^+$ and hydrogen peroxide in buffer pH 6–7 in the absence of the substrate OPD. Under these more challenging conditions methionine gave a low conversion to sulfoxide after 2 h.

25 (*a*) W. Kaim and B. Schwederski, *Bioinorganic Chemistry: Inorganic Elements in the Chemistry of Life*, John Wiley, N.Y., 1994, p. 109; (*b*) In general redox couples with high spin Fe(II) such as $Fe_{(aq)}^{3+}/Fe^{2+}_{(aq)}$ are lower than couples with low spin $[Fe(bipy)_3]^{2+}$ due to the increased stabilization of the d^6 electronic configuration of Fe(II) compared to the d^5 electronic configuration of Fe(III) in a strong field (low spin) system. The [Fe^{II}(**BP1**)] is not a strong field complex, therefore this contribution is missing and the redox potential of the [Fe^{III}(**BP1**)]/[Fe^{II}(**BP1**)] couple is expected to be lower than the redox potential of $[Fe(bipy)_3]^{2+}$.

26 M. van de Heuvel, T. A. van den Berg, R. M. Kellogg, C. T. Choma and B. L. Feringa, *J. Org. Chem.*, 2004, **69**, 250–262.

